



Viscous anisotropy of two-phase composites, and applications to rocks and structures

Susan H. Treagus*

Department of Earth Sciences, University of Manchester, Manchester M13 9PL, UK

Accepted 19 June 2003

Abstract

Anisotropy of viscosity in rocks has a significant effect on the development of geological structures, as demonstrated in several theoretical and analogue model studies. This paper develops the results of a self-consistent mechanics approach to modelling the bulk viscous properties of two-phase composites, to reveal the strength of the viscous anisotropy. Anisotropy factor, δ , is defined as the ratio of normal to shear viscosity, μ_N/μ_S . The value of δ is determined for different types of composites of two viscous phases with varying viscosity ratio ($m=5, 10, 100$), ranging from bilaminates to those with elliptical shape fabrics given by axial ratio, R . Bilaminates with equal layer thickness are the most highly anisotropic systems, where δ simply depends on m .

These results are applied to rocks, modelled as two-phase composites of competent and incompetent lithologies, with the aim of quantifying the viscous anisotropy that is associated with natural rock deformation and the formation of geological structures. It is deduced that $m=5$ or 10 is an appropriate maximum viscosity contrast for many metasedimentary rocks (e.g. psammite/pelite composites), but that $m=100$ might be effectively reached in limestone/marl pairs, or in rocks containing surfaces of slip or zones of recrystallisation or grain-boundary sliding. These m values give rise to maximum δ values of 3, 5.5 and 25.5, respectively. An anisotropy factor of $\delta \gg 25$ is effectively a composite of a rigid and a viscous phase, and may only be achieved in solid–melt mixtures.

Anisotropic rocks, whether layered or containing a strong shape fabric, will develop folds more easily than isotropic rocks. Characteristic structures are similar folds, chevron folds, kink bands and shear bands. Geometric features of folds, especially fold angularity, may provide methods of quantifying the viscous anisotropy of rocks and composites.

© 2003 Elsevier B.V. All rights reserved.

Keywords: Anisotropy; Viscosity; Two-phase composites; Folds

1. Introduction

Anisotropy of material properties such as viscosity is likely to play an important role in the development of structures in naturally deformed rocks.

Rocks may behave anisotropically because they have a strong fabric (shape and/or crystallographic preferred orientation), or because of repetitive layering that has different mechanical properties. Materials or rocks can be considered statistically homogeneous anisotropic media, if the scale of layering or shape fabric is small relative to the scale of deformation considered. A number of studies have revealed the influence of elastic or viscous anisotropy on fold

* Tel.: +44-161-275-3822; fax: +44-161-275-3947.

E-mail address: s.treagus@man.ac.uk (S.H. Treagus).

initiation and development (Bayly, 1964, 1970; Biot, 1965a,b; Cobbold et al., 1971; Cobbold, 1976; Cosgrove, 1976; Latham, 1979, 1985a,b; Casey and Huggenberger, 1985; Weijermars, 1992; Hudleston et al., 1996; Fletcher and Pollard, 1999), but derivations of numerical values that characterise the strength of anisotropy in natural rocks are much rarer.

This paper will investigate the degree of viscous anisotropy in various types of two-phase viscous composites ranging from layered to particulate (Fig. 1), with the aim of bracketing possible values of anisotropy in crustal rocks. Following Honda (1986), Weijermars (1992) and Mandal et al. (2000), the anisotropy will be described throughout by *anisotropy factor*, δ , the ratio between the viscosity under normal stress and viscosity under shear stress, i.e. $\delta = \mu_N/\mu_S$. It is equivalent to A of Hudleston et al. (1996), and is analogous to elastic anisotropy factor, N/Q of Biot (1965a), Cobbold (1976) and others. The δ value is a useful index of anisotropy in two dimensional analyses of two-phase media, such as the cross sections shown in Fig. 1, that are statistically homogeneous, orthotropic (Biot, 1965a) and transversely isotropic. More terms are needed to define the anisotropy of composites with three-dimensional shape fabrics (Mandal et al., 2000), or nonlinearly viscous composites, which will not be considered in this paper.

With the exception of Mandal et al. (2000), most analyses of anisotropy have concerned layer-type anisotropy, the bilaminate model. If an anisotropic viscous medium is considered to comprise thin alternating layers of two isotropic viscous phases with viscosities of μ_1 and μ_2 , its normal and shear viscosities (μ_N , μ_S) are given by:

$$\mu_N = \alpha_1 \mu_1 + \alpha_2 \mu_2 \quad (1a)$$

$$\mu_S = 1/\{\alpha_1/\mu_1 + \alpha_2/\mu_2\} \quad (1b)$$

(Biot, 1965a, p. 432), where α_1 and α_2 are the phase area fractions ($\alpha_1 + \alpha_2 = 1$). Denoting the viscosity ratio $\mu_2/\mu_1 = m$, the anisotropy factor ($\delta = \mu_N/\mu_S$) of this bilaminate is written:

$$\delta = (\alpha_1 + \alpha_2 m)(\alpha_1 + \alpha_2/m) \quad (2)$$

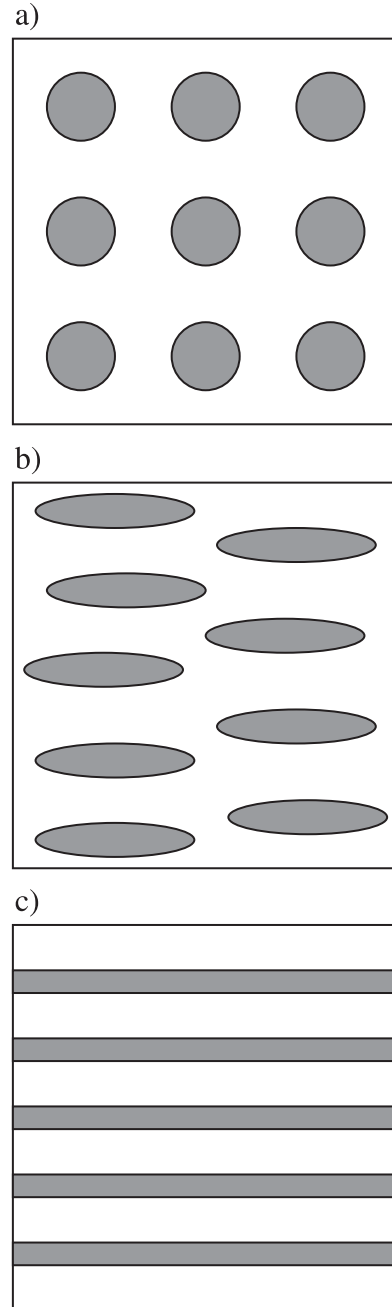


Fig. 1. Schematic representation of three types of two-phase mixture in two-dimensional section. A nominal competent phase is shaded, the incompetent phase is white, and the competent fraction is ~ 0.25 . (a) Circular clasts in a matrix (circular cylinders in 3D). (b) Elliptical clasts in a matrix, with ellipse axial ratio (R) of five (elliptical cylinders in 3D). (c) Bilaminate multilayer, also representing infinitely elliptical clasts in a matrix.

This is a symmetric function, such that δ for α_2 equals δ for $(1 - \alpha_2)$. Maximum δ is at $\alpha_1 = \alpha_2 = 0.5$, simply expressed as:

$$\delta_{\max} = (m + 1)^2 / 4m \quad (3)$$

For high viscosity contrasts (where $m > 100$), δ_{\max} approximates to $m/4$.

What values of viscosity ratio (m) are appropriate to use for modelling two-phase rocks? Talbot (1999) reviews some of the methods by which rock viscosity and viscosity contrasts have been measured, using structures such as folds, mullions and boudins. He determined values for some metamorphic and igneous rocks, and focused on changes of viscosity with pressure and temperature, and between solid rocks and melts. Using dominant wavelengths of folds, and application of Fletcher and Sherwin (1978), Talbot determined m values in the range of 5 to 20 for quartz veins relative to pelitic gneiss. These are comparable to values of 15 to 20 determined by Sherwin and Chapple (1968) for folded quartz veins in phyllite or slate, whereas Hara and Shimamoto (1984) calculated m values of 94–136 for quartz veins in pelitic schist, 23–33 for quartz veins in psammitic schist, and 14–26 for quartz veins in basic schist. Some of the differences between these three studies may reflect the methods of analysis, but they are more likely to be indicative of real differences in the rheology of pelites, schists and gneisses (also quartz) for the different data sets. From these three studies of folded quartz veins, an approximate value of $m = 20$ might be taken for the viscosity ratio of vein quartz to ‘pelite’ at low to moderate metamorphic grade. This might be an appropriate value for modelling the viscosity ratio between quartz-rich and mica-rich laminae in a phyllite (cf. Bayly, 1970), but not necessarily for viscosity contrasts among sedimentary rock layers or clasts, such as sandstone/shale alternations. In their high amplitude modelling of folds in the Appalachians, Cruikshank and Johnson (1993, Table 1) have assumed viscosity ratios of 100 (relative to shale) for massive sandstone formations, and 20 to 30 for intermediate formations.

Studies of cleavage refraction in metasedimentary rocks (Treagus, 1999) estimated effective viscosity contrasts of ~ 5 for psammites relative to pelites. Recent analyses of conglomerates (Treagus and Treagus,

2002, and references therein), concluded that the viscosity contrasts among pelites, psammites, volcanics, quartzites and granites encompass about one order of magnitude only. Thus, when modelling the competent/incompetent viscosity contrasts among sedimentary or low-grade metamorphic rocks, $m = 5$ or 10 would seem sufficient, contradicting the higher values used by Cruikshank and Johnson (1993). However, in rock multilayers that contain surfaces of slip (e.g. Chapple and Spang, 1974), where the slip surfaces can be modelled as vanishingly thin incompetent layers of low viscosity, the competent/incompetent viscosity ratio might reach two or more orders of magnitude. Much larger m values (>100) would be expected in rocks that deformed as solid–melt layers or mixtures (Honda, 1986; Talbot, 1999).

With these values and Eq. (3) in mind, it is appropriate to review what values of anisotropy (δ) have been adopted in previous structural modelling and applications to rocks, and what have been considered “high” and “low” anisotropy. The results of Bayly’s analyses of folds in phyllite (Bayly, 1970) cannot be simply written as a multilayer δ , because he obtained relative viscosity values in a bilaminate comprising an isotropic later (simulating quartz-rich) alternating with anisotropic layers (simulating mica-rich); the anisotropy of the latter was deduced to be >12.5 . His value ranges produce a δ value for the rock as a whole (phyllite) of >12 . Chapple and Spang (1974) found that a model with $\delta = 29$ best fitted their field data for a fold in layered limestone with bedding-parallel slip. Cobbold (1976) illustrated fold shapes for values of $\delta = 1, 2, 5$ and ∞ , thus covering the whole value range. Casey and Huggenberger (1985) adopted an anisotropy factor equivalent to $\delta = 33.3$ to model similar folding in interbedded limestones and marls, and Casey and Williams (2000) again used $\delta = 33.3$, this time to simulate the anisotropy of quartz mylonites. Weijermars (1992) considered values of $\delta = 100$ as a high value of anisotropy. Hudleston et al. (1996) used $\delta = 5$ and 50 (for high and low anisotropy) in finite-element models of folding anisotropic single layers. Fletcher and Pollard (1999) used values of 1, 2, 4, 8, 16 and 128, and suggested $\delta = 8$ was a moderate anisotropy. Mühlhaus et al. (2002) mostly used $\delta = 10$ for finite-element models of folding in anisotropic viscous and visco-elastic layers.

Limited information on anisotropy of creep in laminar rocks does not support the idea that these rocks are very highly anisotropic. Shear and Kronenberg (1993) estimated the strength anisotropy of foliated rocks (mainly schists), and found that the ratio of strength parallel and 45° to the foliation was generally <2 . In the classic laboratory deformation of phyllite, Paterson and Weiss (1966) revealed anisotropy in yield strength of 2 to 3. Although anisotropy of strength may not be comparable with anisotropy of viscosity, these values would suggest that viscous anisotropy may be surprisingly small in schistose rocks. Hudleston et al. (1996) reviewed the evidence for quartz, and concluded that $\delta=10$ might be the highest value of viscous anisotropy in a quartz mylonite.

The present paper will quantify the viscous anisotropy in idealised two-phase media ranging from layered to particulate (Fig. 1), to determine likely values for this type of anisotropy in natural rocks of

different kinds. It forms a sequel to a recent study of the bulk viscosity of two-phase media of different types (Treagus, 2002) which revealed their anisotropy, and its relationship to the shape fabric of the composite, but did not attempt to quantify this property. This paper offers a complementary approach to that of Mandal et al. (2000), who determined anisotropy factors (δ) in media with anisotropic shape fabrics modelled as arrays of rigid inclusions in a viscous matrix. The results will be compared and discussed in a later section.

2. Viscosity of two-phase composites, and degree of anisotropy, δ

The simplest kind of two-phase composite is a bilaminate multilayer, as discussed above, whose anisotropy was revealed in Eqs. (1a), (1b), (2) and (3). However, a wide range of two-phase composites

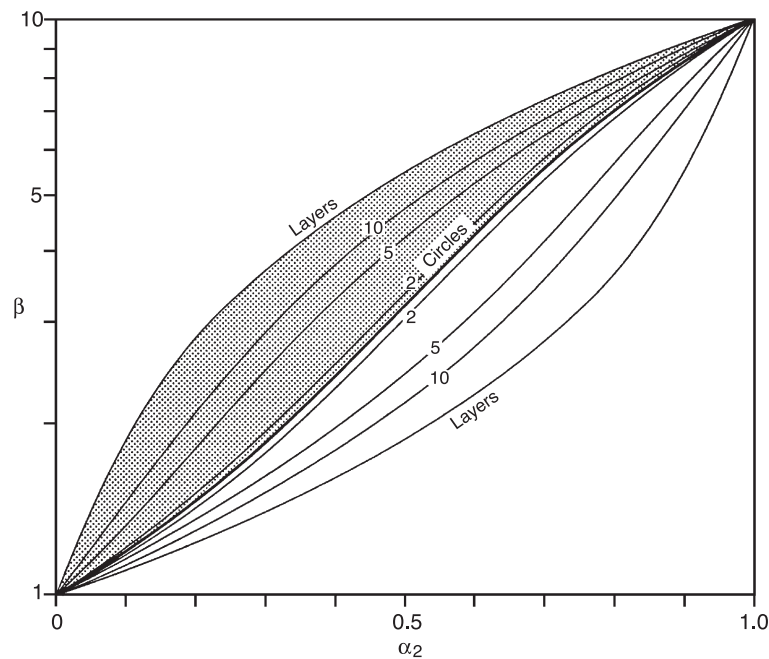


Fig. 2. Bulk rheology graph, after Treagus (2002, Fig. 7), illustrating the change in normalised bulk viscosity β ($=\mu^*/\mu_1$) with competent phase fraction (α_2) and ellipse axial ratio, R (numbered curves), for a two-phase viscosity contrast of $m=10$. The bold central curve indicates isotropic bulk viscosity, for the composite comprising circular clasts ($R=1$). The stippled upper graph region indicates normal viscosity ($\beta_N=\mu_N/\mu_1$) parallel/perpendicular to the shape fabric. The lower unshaded region indicates shear viscosity ($\beta_S=\mu_S/\mu_1$). The upper and lower curves are the ‘bounds’ discussed in the text, and indicate β_N and β_S for layers (bilaminate).

of Newtonian viscous fluids with coherent interfaces were modelled by Treagus (2002), demonstrating that systems with different types of shape fabric (Fig. 1) have different bulk viscosities. The solutions were obtained by application of the method of “self-consistent mechanics” (Hill, 1965; Budiansky, 1965; Hashin, 1983), combined with the Eshelby model of a circular (cylindrical) inclusion in a matrix (Eshelby, 1957; Bilby et al., 1975). For two-dimensional composites of aligned elliptical objects in a matrix (e.g. Fig. 1b), Treagus (2002) demonstrated that the bulk viscosity (μ^*) for deformation parallel to the fabric varies with (i) the viscosity contrast between the two viscous (Newtonian) phases ($m = \mu_2/\mu_1$), (ii) the phase fractions ($\alpha_1 + \alpha_2 = 1$), and (iii) a ‘shape factor’ term (p), related to the ellipticity of the fabric.

The following quadratic equation (Treagus, 2002) describes the normalised bulk viscosity, μ^* , in any homogeneous two-dimensional mixture or composite in deformation parallel to the fabric:

$$p\mu^{*2} + \{(\mu_1 + \mu_2) - (1 + p)(\alpha_1\mu_1 + \alpha_2\mu_2)\} \times \mu^* - \mu_1\mu_2 = 0 \quad (4)$$

This equation can be more simply written in terms of the bulk viscosity normalised to the incompetent phase, β ($= \mu^*/\mu_1$), the two-phase viscosity ratio (m), the stiffer fraction (α_2), and p , as:

$$p\beta^2 + \{(m - p) - \alpha_2(m - 1)(1 + p)\}\beta - m = 0 \quad (5)$$

This is the critical equation from which the anisotropy factor of each composite can be derived.

When $1 < p < \infty$, positive roots of Eq. (5) are the normalised normal viscosity of the composite ($\beta_N = \mu_N/\mu_1$, with $\mu_N = \mu^*$), in a direction parallel/perpendicular to the shape fabric. Here, p has the following relationship to the axial ratio, R of the elliptical fabric:

$$p = (R^2 + 1)/2R \quad (6)$$

(Treagus, 2002). Thus, for $R = 1$, $p = 1$ (Fig. 1a); for $R = 5$, $p = 2.6$ (Fig. 1b); for $R = \infty$, i.e. layers, $p = \infty$ (Fig. 1c). Fig. 2 illustrates solutions for composites with $m = 10$; curves of β_N are in the shaded upper region, numbered for ellipses with different R values.

The uppermost curve, representing a bilaminate ($R = \infty$, $p = \infty$), is the upper bound for the bulk viscosity of any two-phase composite, representing uniform strain rate. It has the linear expression:

$$\mu^* = \alpha_1\mu_1 + \alpha_2\mu_2 \quad (7)$$

which is the solution to Eq. (4) when $p = \infty$, and is identical to the expression for μ_N in a bilaminate given earlier (Eq. (1a)). It normalises to:

$$\beta_N = 1 + \alpha_2(m - 1) \quad (8)$$

When $0 < p < 1$, positive roots of Eq. (5) are the normalised shear viscosity of the composite ($\beta_S = \mu_S/\mu_1$, with $\mu_S = \mu^*$), in a direction parallel/perpendicular to the shape fabric. Now, p takes inverse values to those for β_N (Eq. (6)):

$$p = 2R/(R^2 + 1) \quad (9)$$

Solutions for β_S are shown in the unshaded lower region of Fig. 2. The lowermost curve, representing a bilaminate ($R = \infty$, $p = 0$), is the lower bound for the

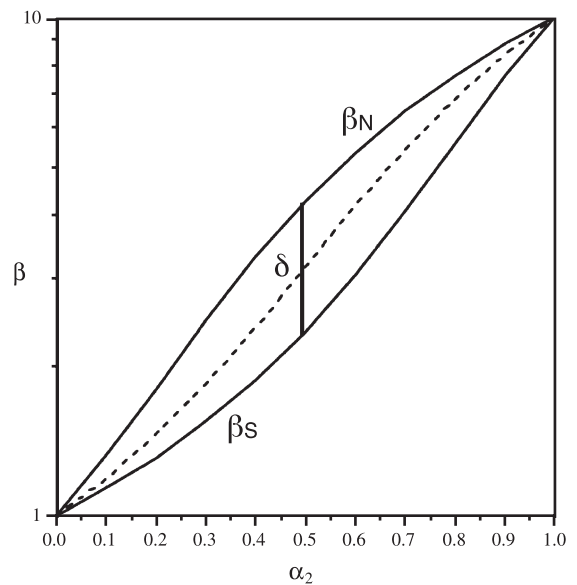


Fig. 3. Normalised normal and shear viscosities (β_N , β_S) for $R = 5$ and $m = 10$ and varying α_2 . The anisotropy factor, δ , is the distance between the curves, shown here in the δ_{max} position at $\alpha_2 = 0.5$. The midway curve for isotropy is dashed.

bulk viscosity of any two-phase composite, representing uniform stress. It has the expression:

$$\mu^* = 1/\{\alpha_1/\mu_1 + \alpha_2/\mu_2\} \tag{10}$$

which is the solution to Eq. (4) when $p=0$, and is identical to the expression for μ_S in a bilaminate (Eq. (1b)). It normalises to:

$$\beta_S = 1/\{(1 - \alpha_2) + \alpha_2/m\} \tag{11}$$

The ‘central’ curve of Fig. 2 shows $\beta_N = \beta_S$ for $p=1, R=1$, demonstrating that a composite of circles in two dimensions (Fig. 1a) has *isotropic viscosity*. Here, Eq. (5) takes the form:

$$\beta^2 + \{(m - 1)(1 - 2\alpha_2)\}\beta - m = 0 \tag{12}$$

The anisotropy of the composites shown in Fig. 2 is illustrated by the difference between upper (β_N) and lower (β_S) curves with the same numbered R value.

This is illustrated in Fig. 3, representing a composite with an elliptical fabric with $R=5$ (as Fig. 1b), a two-phase viscosity contrast of $m=10$, and varying fraction of the stiffer phase (α_2). The β_N curve is the solution to Eq. (5) for $p=2.6$, and the β_S curve is the solution for $p=0.39$. The *anisotropy factor*, δ , is given by $\delta = \mu_N/\mu_S = \beta_N/\beta_S$. Because these viscosity graphs are drawn on a log scale, δ is the ordinate distance between the β_N and β_S curves in Fig. 3. This useful feature allows a graphical appreciation of the values of viscous anisotropy for a wide range of two-phase media, in terms of the phase fractions, their viscosity contrasts and their shape fabric. An immediate result, apparent in Fig. 3, is that the maximum anisotropy occurs for equal phase fractions ($\alpha_1 = \alpha_2 = 0.5$). This is true for all examples of specially orthotropic media (Cobbold, 1976), whether comprising layers or elliptical clasts.

It is demonstrated in Fig. 2 that the most anisotropic two-phase composite is a bilaminate. Thus, the maximum possible value of δ in a composite with

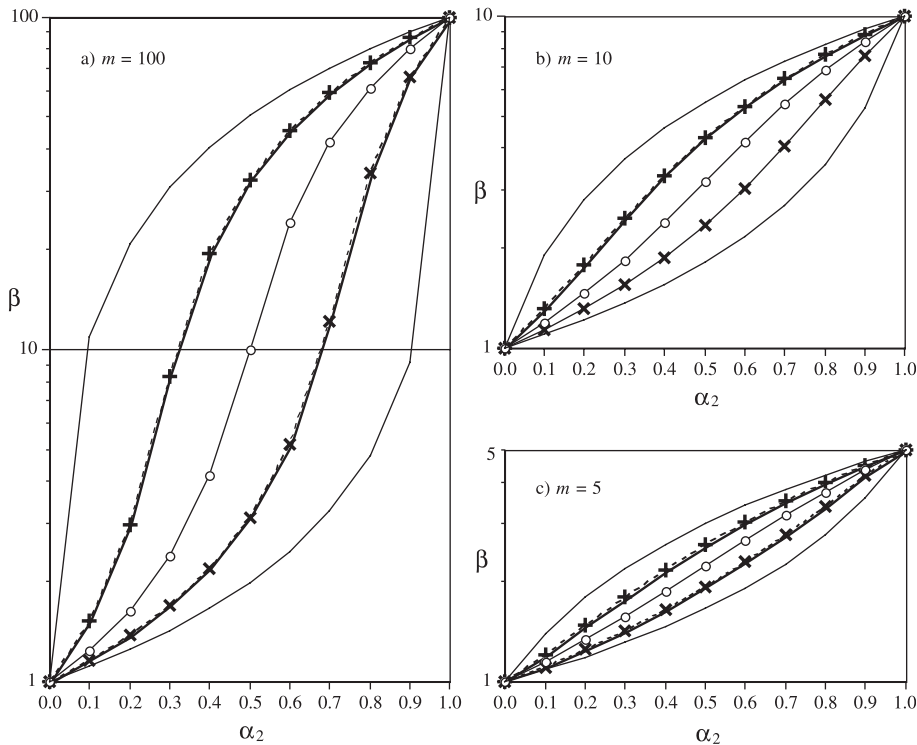


Fig. 4. More examples (on the design of Figs. 2 and 3), showing the variation of β with fabric. Central dotted curves show isotropic viscosity, β , for circular clasts. Curves with crosses show β_N (upper curve) and β_S (lower curve) for $R=5$. The solid curves show the upper and lower bounds for a bilaminate ($R = \infty$). (a) Two-phase viscosity contrast, $m=100$; (b) $m=10$; (c) $m=5$.

two-phase viscosity contrast, m , is as given in Eq. (3). The approximation of $\delta_{\max} \cong m/4$ is useful, where $m \geq 100$.

All the derivations and results in this section, developed from Treagus (2002), apply to deformation of composites orthogonal to the aligned fabric, where $\beta_N \geq \beta_S$, and $\delta \geq 1$. If composites of the kind shown in Fig. 1 are deformed 45°-diagonal to their shape fabric, the two principal viscosities now have the relationship, $\beta_N \leq \beta_S$. (Values for β_N in the diagonal composite are equivalent to β_S in the aligned composite, and vice versa; Treagus, 2002.) These composites have reciprocal δ values to those derived above (and next), in the range of ≤ 1 .

3. Results: values of δ for different two-phase composites

Some further examples are given in Fig. 4 of the β values for composites that comprise circular

clasts, elliptical clasts with $R=5$, and bilaminate layers ($R=\infty$), with two-phase viscosity contrasts of $m=100$, 10 and 5. According to the introductory review, these m values probably cover realistic ranges for two-phase viscosity ratios expected in different types of rocks. It was shown in Treagus (2002) that an $m=100$ composite is a reasonable approximation to a system with rigid clasts in a viscous matrix ($m=\infty$), whereas m values of 5 or 10 may be sufficient when modelling metasedimentary rocks as two-phase composites.

Exact values of δ for the examples in Fig. 4 are shown in Fig. 5, revealing the symmetry in δ values with phase fraction (α_1 or α_2). In other words, a composite that comprises 0.2 fraction (20%) of the stiffer phase will have exactly the same value of anisotropy as a composite with 0.2 fraction of the less viscous phase. Fig. 5 demonstrates that maximum δ values are always at $\alpha_2=0.5$. The variation of δ with phase fractions (α_2) is particularly striking for the high viscosity contrast system ($m=100$) shown in Fig. 5a,

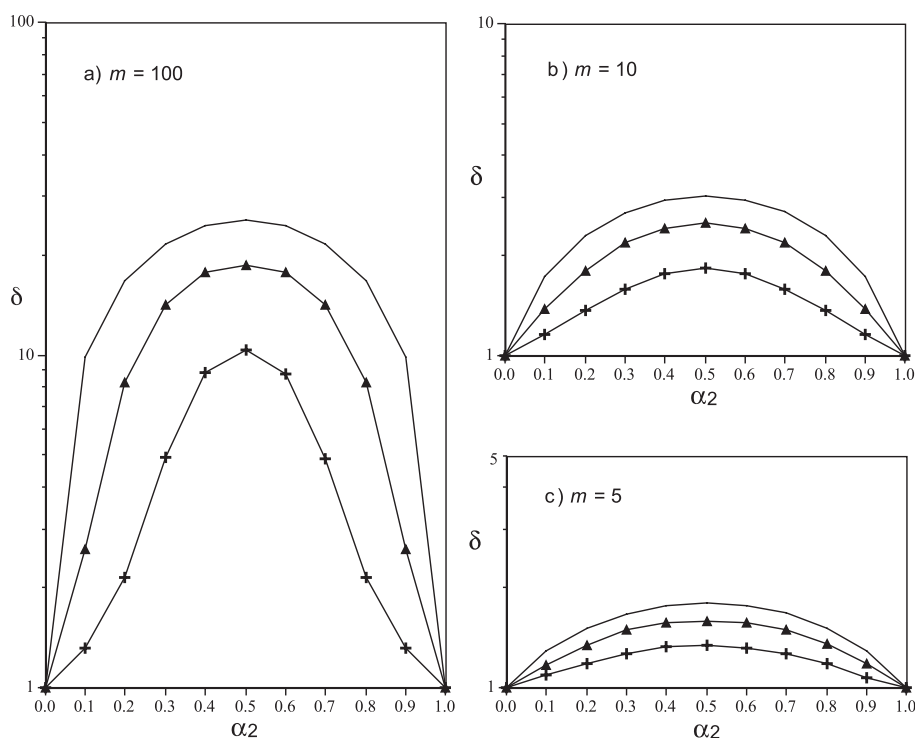


Fig. 5. Values of anisotropy factor, $\delta = \mu_N/\mu_S$, determined for the examples in Fig. 4 (same symbols), plus $R=18$ (triangles). Note the symmetry with α_2 (or α_1).

especially for layers and strongly elliptical fabrics. Although the anisotropy is highest for equal layer thicknesses ($\delta_{\max} = 25.5$ at $\alpha_2 = 0.5$), δ is a similar value for approximately equal thicknesses ($0.4 < \alpha_2 < 0.6$). However, for systems with a small to moderate phase viscosity contrast of $m = 5$ or 10 (Fig. 5b,c), δ only gently increases with α_2 or α_1 , to δ_{\max} at $\alpha_2 = \alpha_1$.

In bilaminates with very unequal layer thicknesses, such as where $\alpha_2 = 0.1$ or 0.9, the anisotropy is relatively weak. This is an interesting result, as the opposite might be expected: that strongly unequal thicknesses of stiffer and weaker layers might make a more anisotropic mixture than mixtures with about equal layer thicknesses. So, despite the flow variations being greatest in a bilaminate multilayer with very unequal layer thicknesses (Treagus, 1993), the viscous anisotropy is not at its highest for such a system. To obtain significant anisotropy for very unequal fractions requires very large m values.

Values of δ_{\max} for different types of composites with $\alpha_1 = \alpha_2 = 0.5$ will now be considered. For a layered medium, δ_{\max} is given in Eq. (3) as a simple relationship with m , which is graphed in Fig. 6. Note its progressive approach to linearity ($=m/4$) as $m \rightarrow 100$. At values of $m = 5$ to 10, δ_{\max} takes values of only ~ 2 to 3. In nonlayered two-phase compo-

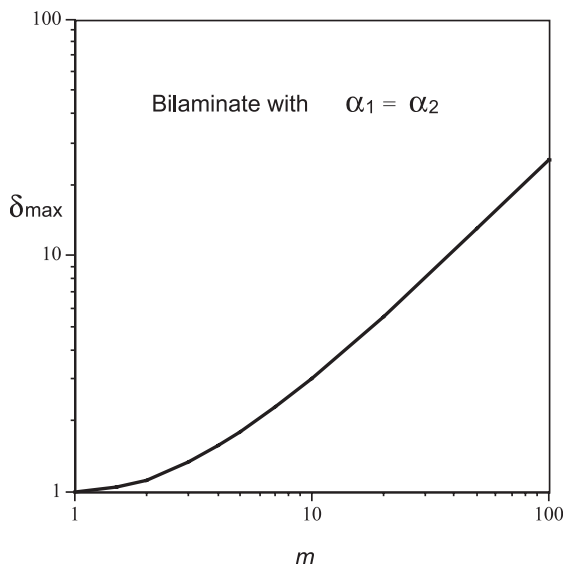


Fig. 6. Value of δ_{\max} for equal layer thickness bilaminates ($\alpha_1 = \alpha_2$), with varying two-phase viscosity contrast, m .

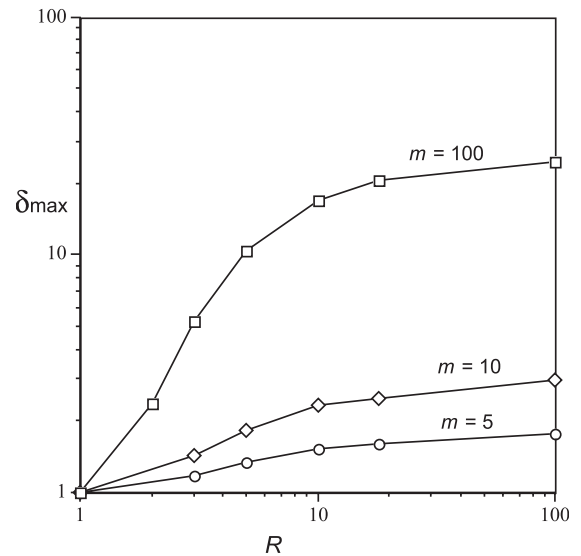


Fig. 7. Value of δ_{\max} ($\alpha_1 = \alpha_2$) for two-phase media with elliptical shape fabrics (R) for two-phase viscosity contrasts of $m = 5, 10$ and 100. Symbols denote calculations for $R = 3, 5, 18$ and 100 (\sim layers).

sites, such as materials with elliptical shape fabrics, δ_{\max} increases with ellipticity, R , as shown in Fig. 7. Where $R = 100$, values of δ_{\max} approach those shown in Fig. 6 for layers. For the high contrast system ($m = 100$), R has a particularly marked effect on δ_{\max} , with $\delta_{\max} > 10$ for $R > 5$. However, for $m = 10$, δ_{\max} values only reach 2.5 for $R = 18$. For $m = 5$, δ_{\max} is < 2 , even for an infinitely elliptical fabric (layers), as also shown in Fig. 6.

4. Discussion and geological implications

4.1. Anisotropy values (δ) for rocks

The results outlined above can be compared with those derived by Mandal et al. (2000) where a composite was modelled as a rigid phase (with linear or planar elliptical fabric) of up to 0.5 fraction, in a viscous phase. Mandal et al. found that the δ values are proportional to the axial ratios (R) of the rigid inclusion fraction (prolate or oblate ellipsoids), and increase nonlinearly with increasing rigid fraction (up to their limit of ~ 0.5), which is also seen in Figs. 5–7. Their media with linear fabrics had δ values of 1 to

4.5 for $R=1$ to 10 and rigid fractions of 0 to 0.5; their media with planar fabrics mostly have a narrower range ($\delta=1-3$), with less sensitivity to the rigid fraction, but reach high δ values when $R>10$. Their result of $\delta=25$ for $R=100$ is almost the same as the value of 25.5 derived for a bilaminate with $m=100$ (Eq. (3)), and for my composite with $m=100$ $R=100$ (Fig. 7). This tends to confirm the conclusion (Treagus, 2002) that an $m=100$ composite is a valid approximation to a composite of a rigid phase in a viscous phase (up to 0.5 rigid fraction).

Figs. 5–7 show that to develop a high anisotropy ($\delta>25$) in a multilayer that is approximated to a bilaminate system requires a viscosity contrast among competent and incompetent layers of $m>100$. This is probably higher than viscosity contrasts effective between alternating sedimentary or metasedimentary rock layers, according to the review in the Introduction. So it would seem that high anisotropy is only achieved where one phase is quasi-rigid in comparison with the other (viscous) phase, and perhaps that they are in roughly equal fractions. This might be the effective behaviour of (a) some alternating rock layers, such as limestone-marl beds (Casey and Huggenberger, 1985), (b) rock layers with planes or zones of slip, such as the folded limestone of Chapple and Spang (1974), or (c) rocks undergoing grain-boundary sliding and sequences of crystallisation/recrystallisation such as the mylonites of Casey and Williams (2000). These scenarios may be the exception, and it seems probable that most lithologies at low to moderate metamorphic grade, even where they contain strong planar fabrics or are foliated or layered, are only weakly anisotropic, with $\delta=3$ or less. Only rocks in partial melting, such as the model for anisotropic asthenosphere by Honda (1986), would seem likely to obtain very high δ values of >100 .

4.2. Folds and anisotropy

Most of the investigations of anisotropy and structures concentrate on folding of anisotropic media with planar anisotropy, modelled as bilaminate multilayers. Rigidly confined anisotropic media in compression develop internal instability of buckling or kinking type (Biot, 1965a; Cobbold et al., 1971; Cosgrove, 1976; Latham, 1979, 1985a,b). Softly confined anisotropic media in compression can fold as a whole (Biot,

1965b), or can develop folds on small and larger wavelengths at the same time (Mühlhaus et al., 2002), and anisotropic layers fold more readily than isotropic layers with the same (normal) viscosity ratio to the embedding medium. The finite shapes of folds in anisotropic layers are controlled by the strength of the anisotropy (Bayly, 1964, 1970; Cobbold, 1976; Casey and Huggenberger, 1985; Fletcher and Pollard, 1999): the higher the anisotropy, the stronger and more angular the folding. The following discussion concentrates on fold features that might be indicative of the degree of anisotropy in rocks.

Internal instabilities in layered anisotropic media that produce folds, kinks and shear bands, have been well documented (Biot, 1965a,b; Cobbold et al., 1971; Price and Cosgrove, 1990). Biot's Type 1 instabilities, internal similar or chevron folds, require values of $\delta>0.5$, and such structures have been produced in many analogue models (e.g. Bayly, 1970, 1971; Cobbold et al., 1971; Latham, 1979). All the two-phase anisotropic media considered in this paper have δ values of >0.5 , when oriented with the fabric parallel to shortening or extension. So they could *all* develop fold instabilities that grow into finite similar to chevron folds, when shortened parallel to the fabric.

For Biot's Type 2 internal instability (kink or shear bands) to arise requires $\delta<0.5$ (Cobbold et al., 1971). It was noted earlier that composites that have δ values of >1 in deformation parallel to their fabric, will have δ values inverted in deformation at 45° to the fabric. (This is because the μ_N and μ_S values are exchanged.) Thus, any material with $\delta>2$ in Figs. 5–7 will have $\delta<0.5$ in its diagonal orientation, and could develop kink or shear-band instabilities oriented diagonal to the anisotropy fabric. For high contrast systems (e.g. two-phase viscosity contrasts of $m=100$), these instabilities will occur in layered systems and in those with elliptical fabrics of $R\geq 5$ (unless the phase fractions are proportionally very different). However, for a more modest competence contrast of $m=10$, $\delta>2$ is only found for approximately equal phase fractions and where $R>7$. Thus, kink and shear-band instabilities should only arise in multilayered media and those with a very strong shape preferred orientation. In practice, it is likely that both types of instability go hand-in-hand, in anisotropic rocks, developing from infinitesimal points of initiation (of Type 1 or 2) into finite structures

forming a spectrum from conjugate folds and kink bands, to chevron to similar folds.

Angularity of folding can provide an index of anisotropy, as demonstrated by Bayly (1964) and Cobbold (1976). Cobbold considered passive development of similar folds from an initial sinusoidal instability within variably anisotropic media. Isotropic media develop similar folds of increasingly high amplitude sinusoidal form, whereas folds in media with anisotropy (δ) of 2 and 5 are progressively more angular, with higher amplitudes. Folding is completely angular for the limiting case of $\delta = \infty$, even though the fold limb dips and amplitudes are not significantly greater than for $\delta = 2$ or 5. The reason for these differences in fold shape, related to the degree of anisotropy, is the non-coaxial relationship of stress and strain in anisotropic media: a supposedly passive shortening of a sinusoidal instability in an anisotropic medium gives rise to heterogeneous deformation, with a greater strain arising through shear strain, that reaches a maximum when layering is at 45° to the compression. Because of the different amounts of rotation that occur for layering or fabric in different orientations to shortening, the sinusoid becomes significantly straightened into almost constant limb dip, as the material anisotropy increases. According to this mechanism, folds of *chevron style* (Ramsay, 1967, 1974) will develop in quite moderately anisotropic media ($\delta > 2$) (Cobbold, 1976).

Fletcher and Pollard (1999) reviewed models of chevron and similar folding and provided a mechanical model for chevron folding in anisotropic media. They demonstrate the change from sinusoid to chevron form in graphs of limb dip versus shortening for different δ values. From these analyses of similar/chevron folding (Bayly, 1964; Cobbold, 1976; Fletcher and Pollard, 1999), in theory, it should be possible to assess the degree of anisotropy in a multilayered medium from the degree of fold angularity, such as the relative widths of limb and hinge zones. The author is not aware that this has ever been done in practice.

Other features of *fold geometry* may also be indicative of anisotropy. Biot (1965b) considered the initiation of two kinds of ‘similar’ folds in multilayers that are statistically anisotropic. The “first kind” is true *parallel folding* (i.e. class 1B geometry, Ramsay

(1967, p. 365), and must satisfy the condition (in the present nomenclature):

$$\mu_S/\mu_M \gg 5\sqrt{\delta} \quad (13)$$

where μ_S is the shear viscosity of the statistically anisotropic layer or multilayer, and μ_M is the viscosity of the embedding medium. The “second kind” is true *similar folding* (class 2 geometry), and must satisfy the condition:

$$\mu_S/\mu_M \ll 5\sqrt{\delta} \quad (14)$$

Each is associated with a characteristic wavelength (Biot, 1965b). Between these extremes, hybrid parallel-similar folds would be expected.

However, finite-element modelling of fold development in anisotropic layers in an incompetent embedding medium (Hudleston et al., 1996; Mühlhaus et al., 2002) does not demonstrate that these two kinds of fold geometry are maintained in the finite fold shapes. According to Eqs. (13) and (14), the $\delta = 5$ model of Hudleston et al. (1996, Fig. 5) should have parallel folds (first kind), whereas $\delta = 50$ should have similar folds. The folds, modelled with the same initial wavelength–thickness relationship ($L/H = 12$), show hardly any difference in their fold geometry: both are approximate parallel folds (class 1B) of sinusoidal shape. The models of Mühlhaus et al. (2002) show the development of sinusoidal folding on two scales ($L/H \approx 12$ and 1.2) for $\delta = 10$ and $\mu_N/\mu_M = 10$ and 100. The larger folds in both models appear close to parallel in geometry, despite the first ($\mu_N/\mu_M = 10$) satisfying Biot’s condition (Eq. (14)) for similar folding. Finite amplitude numerical models by Johnson and Fletcher (1994, p. 351) of a softly embedded 17-layer multilayer, that has $\delta \approx 3$ and satisfies Eq. (14), are also not perfect similar folds, but of Ramsay’s class 1C geometry. Therefore, it is not presently clear how closely the finite fold geometry of an anisotropic layer (or whole multilayer), or the fold class, might reflect the anisotropy factor, δ .

Mühlhaus et al. (2002) demonstrate that anisotropic layers fold at smaller viscosity contrasts (relative to embedding medium) than for isotropic layers. For example, weak folding can even arise in an anisotropic layer where $\mu_N/\mu_M = 1$. They also show that where $\delta = 10$ and $\mu_N/\mu_M = 100$, folds of two wavelengths can

develop at the same time, as ‘wrinkles’ and larger folds. Although such a high viscosity contrast between anisotropic layer and embedding medium might be unlikely in rocks, these models provide a possible explanation for folding on different scales. For example, a schist layer that contains a pre-existing foliation might fold as a whole layer, and at the same time be crenulated on the scale of the schistosity, to create a crenulation cleavage (Cosgrove, 1976).

Folding mechanism has been related to anisotropy by Price and Cosgrove (1990, p. 250), and Weijermars (1992), who stated that strongly anisotropic single layers are more likely to fold by a mechanism of *flexural flow* (layer-parallel simple shear), than by tangential longitudinal strain (layer-parallel pure shear) (cf. Ramsay, 1967, pp. 391, 398). Weijermars concluded that a layer with a high anisotropy ($\delta = 100$) would fold in perfect flexural flow. Hudleston et al. (1996) examined this premise via finite element models, to reveal that a viscous anisotropy of $\delta > 50$ was required to produce effective flexural flow in a single anisotropic layer. They concluded that competent rock layers would be unlikely to possess such a high degree of anisotropy. Alternating competent and incompetent layers that behave as a statistically anisotropic ‘single’ layer would need to have competent/incompetent viscosity contrasts of $m \cong 200$ to attain $\delta \cong 50$, and thus to have a bulk folding mechanism close to flexural flow. Such high m and δ values seem unlikely for many metasedimentary rocks, as discussed earlier.

4.3. Anisotropy and structures in progressive deformation

Consider, now, a two-phase medium or rock in progressive deformation. If it begins as an *isotropic* mixture of clasts, a pure shear deformation creating a strain shape fabric would make it progressively more anisotropic, with the anisotropy tensor parallel to the deformation tensor. It will be stiffer in longitudinal stress and weaker in shear stress, as shown in Fig. 2. Assuming the material does not change its phase fractions, it will progressively depart from the central curve (isotropy) along ordinate lines in Fig. 2, tracking values related to the developing elliptical fabric. Thus, in pure shear, the material remains specially orthotropic (Cobbold, 1976). Extension will always

be parallel to the developing anisotropy, and extensional structures characteristic of anisotropic systems could develop: e.g. pinch and swell or extensional kinking, extensional shears and crenulations, or foliation boudinage (Cobbold et al., 1971; Hanmer, 1979; Platt and Vissers, 1980).

A material with an *initial shape fabric* or a layered fabric, if deformed in pure shear parallel to the fabric, also remains specially orthotropic. In some configurations, the shortening may first act to decrease the fabric and anisotropy. In fabric-parallel shortening, deformation will almost certainly result in internal folding, of conjugate kink to chevron or similar style, as described earlier. Layered systems in extension will also develop internal instabilities, manifested as the extensional features noted above.

The progressive deformation of materials with anisotropy in other orientations to stress or strain is more complex (Cobbold, 1976; Weijermars, 1992). If the principal directions of the anisotropy tensor do not coincide with those of the deformation tensor, the effects are more difficult to generalise. Stresses and strains will not generally be parallel, and the greater the anisotropy, the greater the dominance of simple shear on the progressive deformation. A pure shear oblique to a shape fabric will generally increase the shape fabric and therefore the material anisotropy, and reduce the angle of obliquity between the fabric and the extension direction, so that extensional instabilities may eventually develop.

It was suggested by Treagus (2002) that two-phase composites in simple shear might undergo cycles of stiffening and softening with progressive deformation and fabric development, and these cycles would go hand-in-hand with changes in the strength of anisotropy, δ . The only stable orientation of a fabric in simple shear is where the fabric or layering is parallel to the shear direction. Materials with initially equant fabrics that develop into elliptical fabrics would cycle in strength and anisotropy during simple shear. Layered materials could develop a variety of structures, according to the degree of orientation of anisotropy and its orientation to the simple shear. Platt (1983) suggested a way of producing progressive refolding in shear zones that possessed a strong planar anisotropy, whereby small fluctuations in the shearing rate could produce passively amplifying folds. Weijermars (1992) suggested that variations in simple shear could

produce similar folds, best seen in passive marker 'layers' at a high angle to the shearing direction. Simple shear of anisotropic media could also give rise to internal instabilities, if the anisotropy is favourably oriented. These could appear as anastomosing S-C fabrics or small shear bands or crenulations of various types, as described in naturally sheared rocks (Berthé et al., 1979; Hanmer, 1979; Platt and Vissers, 1980; Lister and Snoke, 1984).

5. Conclusions

The viscous anisotropy of mixtures of competent and incompetent rock phases is dependent on the viscosity contrast of the phases, the phase fractions, and the shape fabric of the material (layered to particulate). The most highly anisotropic systems are bilaminate multilayers with equal layer thickness. For the wide variety of rocks that have an effective competent/incompetent viscosity contrast (m) of 10 or less, then the maximum possible anisotropy (δ) is ~ 3 . Some rocks may deform as two-phase systems with effective $m \approx 100$, and can achieve $\delta \approx 25$, which is close to a model of a quasi-rigid phase and a viscous phase. This may be an appropriate model for rocks containing planes or zones of slip, recrystallisation or grain-boundary sliding. Only where there are orders of magnitude of viscosity contrast, such as expected in solid–melt composites, will much higher values of anisotropy ($\delta > 100$) be achieved (if the system is layered).

Anisotropic rocks develop characteristic deformation structures, such as kink and chevron folds, similar folds and shear bands. For quite small values of anisotropy ($\delta = 2$ or more), significantly angular chevron-style folds may progressively develop from sinusoidal instabilities. All these fold and banded structures may not just be associated with regularly multilayered or foliated rocks, but could also occur in strongly deformed conglomerates or any rocks possessing a strong shape-preferred orientation.

Acknowledgements

This work was undertaken during the tenure of a NERC Senior Research Fellowship, which is grate-

fully acknowledged. I appreciate many helpful comments from Ray Fletcher and Stefan Schmalholz, which led to improvements of the paper.

References

- Bayly, M.B., 1964. A theory of similar folds in viscous materials. *American Journal of Science* 262, 753–766.
- Bayly, M.B., 1970. Viscosity and anisotropy estimates from measurements on chevron folds. *Tectonophysics* 9, 459–474.
- Bayly, M.B., 1971. Similar folds, buckling and great circle patterns. *Journal of Geology* 79, 110–118.
- Berthé, D., Choukroune, P., Jegouzo, P., 1979. Orthogneiss, mylonite and non-coaxial deformation of granites: the example of the South Armorican Shear Zone. *Journal of Structural Geology* 1, 31–42.
- Bilby, B.A., Eshelby, J.D., Kundu, A.K., 1975. The change of shape of a viscous ellipsoidal region embedded in a slowly deforming matrix having a different viscosity. *Tectonophysics* 28, 265–274.
- Biot, M.A., 1965a. *Mechanics of Incremental Deformations*. Wiley, New York.
- Biot, M.A., 1965b. Theory of similar folding of the first and second kind. *Geological Society of America Bulletin* 76, 251–258.
- Budiansky, B., 1965. On the elastic moduli of some heterogeneous materials. *Journal of the Mechanics and Physics of Solids* 13, 223–227.
- Casey, M., Huggenberger, P., 1985. Numerical modelling of finite-amplitude similar folds developing under general deformation histories. *Journal of Structural Geology* 7, 103–114.
- Casey, M., Williams, D., 2000. Micromechanical control of rheological anisotropy in quartz mylonites. *Physics and Chemistry of the Earth* 25, 127–132.
- Chapple, W.M., Spang, J.H., 1974. Significance of layer-parallel slip during folding of layered sedimentary rocks. *Geological Society of America Bulletin* 85, 1523–1534.
- Cobbold, P.R., 1976. Mechanical effects of anisotropy during large finite deformations. *Bulletin Société Géologie France* 7, 1497–1510.
- Cobbold, P.R., Cosgrove, J.W., Summers, J.M., 1971. Development of internal structures in deformed anisotropic rocks. *Tectonophysics* 12, 23–53.
- Cosgrove, J.W., 1976. The formation of crenulation cleavage. *Journal of the Geological Society* 132, 155–178.
- Cruikshank, K.M., Johnson, A.M., 1993. High amplitude folding of linear-viscous multilayers. *Journal of Structural Geology* 15, 79–94.
- Eshelby, J.D., 1957. The determination of the elastic field of an ellipsoidal inclusion, and related problems. *Proceedings of the Royal Society A* 241, 376–396.
- Fletcher, R.C., Pollard, D.D., 1999. Can we understand structural and tectonic processes and their products without appeal to complete mechanics? *Journal of Structural Geology* 21, 1071–1088.
- Fletcher, R.C., Sherwin, J.-A., 1978. Arc lengths of single layer

- folds: a discussion of the comparison between theory and observation. *American Journal of Science* 278, 1085–1098.
- Hanmer, S.K., 1979. The role of discrete heterogeneities and linear fabrics in the formation of crenulations. *Journal of Structural Geology* 1, 81–91.
- Hara, I., Shimamoto, T., 1984. Folds and folding. In: Uemura, T., Mizutani, S. (Eds.), *Geological Structures*. Wiley, Chichester, pp. 191–243.
- Hashin, Z., 1983. Analysis of composite materials—a survey. *Journal of Applied Mechanics* 50, 481–505.
- Hill, R., 1965. A self-consistent mechanics of composite materials. *Journal of the Mechanics and Physics of Solids* 13, 213–222.
- Honda, S., 1986. Strong anisotropic flow in a finely layered asthenosphere. *Geophysical Research Letters* 13, 1454–1457.
- Hudleston, P.J., Treagus, S.H., Lan, L., 1996. Flexural flow folding: does it occur in nature? *Geology* 24, 203–206.
- Johnson, A.M., Fletcher, R.C., 1994. *Folding of Viscous Layers*. Columbia Univ. Press, New York.
- Latham, J.-P., 1979. Experimentally developed folds in a material with a planar mineral fabric. *Tectonophysics* 57, T1–T8.
- Latham, J.-P., 1985a. The influence of nonlinear material properties and resistance to bending on the development of internal structures. *Journal of Structural Geology* 7, 225–236.
- Latham, J.-P., 1985b. A numerical investigation and geological discussion of the relationship between folding, kinking and faulting. *Journal of Structural Geology* 7, 237–249.
- Lister, G.S., Snoke, A.W., 1984. S-C mylonites. *Journal of Structural Geology* 6, 617–638.
- Mandal, N., Chakraborty, C., Samanta, S.K., 2000. An analysis of anisotropy of rocks containing shape fabrics of rigid inclusions. *Journal of Structural Geology* 22, 831–839.
- Mühlhaus, H.-B., Moresi, L., Hobbs, B., Dufour, F., 2002. Large amplitude folding in finely layered viscoelastic rock structures. *Pure and Applied Geophysics* 159, 2311–2333.
- Paterson, M.S., Weiss, L.E., 1966. Experimental deformation and folding in phyllite. *Geological Society of America Bulletin* 77, 343–374.
- Platt, J.P., 1983. Progressive refolding in ductile shear zones. *Journal of Structural Geology* 5, 619–622.
- Platt, J.P., Vissers, R.L.M., 1980. Extensional structures in anisotropic rocks. *Journal of Structural Geology* 2, 397–410.
- Price, N.J., Cosgrove, J.W., 1990. *Analysis of Geological Structures*. Cambridge Univ. Press, Great Britain.
- Ramsay, J.G., 1967. *Folding and Fracturing of Rocks*. McGraw-Hill Book, New York.
- Ramsay, J.G., 1974. Development of chevron folds. *Geological Society of America Bulletin* 85, 1741–1754.
- Shea Jr., W.T., Kronenberg, A.K., 1993. Strength and anisotropy of foliated rocks with varied mica content. *Journal of Structural Geology* 15, 1097–1121.
- Sherwin, J.-A., Chapple, W.M., 1968. Wavelengths of single-layer folds: a comparison between theory and observation. *American Journal of Science* 226, 167–179.
- Talbot, C.J., 1999. Can field data constrain rock viscosities? *Journal of Structural Geology* 21, 949–957.
- Treagus, S.H., 1993. Flow variations in power-law multilayers: implications for competence contrasts in rocks. *Journal of Structural Geology* 15, 423–434.
- Treagus, S.H., 1999. Are viscosity ratios measurable from cleavage refraction? *Journal of Structural Geology* 21, 895–901.
- Treagus, S.H., 2002. Modelling the bulk viscosity of two-phase mixtures in terms of clast shape. *Journal of Structural Geology* 24, 57–76.
- Treagus, S.H., Treagus, J.E., 2002. Studies of strain and rheology of conglomerates. *Journal of Structural Geology* 24, 1541–1567.
- Weijermars, R., 1992. Progressive deformation of anisotropic rocks. *Journal of Structural Geology* 14, 723–742.